The Key Role of Coupled Chemistry–Climate Interactions in Tropical Stratospheric Temperature Variability

SIMCHAN YOOK AND DAVID W. J. THOMPSON

Department of Atmospheric Science, Colorado State University, Fort Collins, Colorado

SUSAN SOLOMON

Department of Earth, Atmospheric, and Planetary Sciences, Massachusetts Institute of Technology, Cambridge, Massachusetts

SEO-YEON KIM

School of Earth and Environmental Sciences, Seoul National University, Seoul, South Korea

(Manuscript received 4 February 2020, in final form 12 June 2020)

ABSTRACT

The purpose of this study is to quantify the effects of coupled chemistry–climate interactions on the amplitude and structure of stratospheric temperature variability. To do so, the authors examine two simulations run on version 4 of the Whole Atmosphere Coupled Climate Model (WACCM): a ''free-running'' simulation that includes fully coupled chemistry–climate interactions and a ''specified chemistry'' version of the model forced with prescribed climatological-mean chemical composition. The results indicate that the inclusion of coupled chemistry–climate interactions increases the internal variability of temperature by a factor of ~2 in the lower tropical stratosphere and—to a lesser extent—in the Southern Hemisphere polar stratosphere. The increased temperature variability in the lower tropical stratosphere is associated with dynamically driven ozone–temperature feedbacks that are only included in the coupled chemistry simulation. The results highlight the fundamental role of two-way feedbacks between the atmospheric circulation and chemistry in driving climate variability in the lower stratosphere.

1. Introduction

The key role of stratospheric chemistry in setting the *climatological-mean* stratospheric circulation is well established. The absorption of shortwave radiation by ozone leads to increasing temperature with height and thus contributes to high values of static stability at stratospheric levels (Brasseur and Solomon 2005). Water vapor contributes to radiative cooling above the extratropical tropopause (Forster and Shine 2002), which leads to the formation of a region of enhanced static stability in the lowermost stratosphere (the tropopause inversion layer; Birner 2006; Randel et al. 2007b). The climatological-mean overturning circulation in the stratosphere is mainly driven by the mixing of potential vorticity by atmospheric waves, but is also influenced by the radiative forcing due to trace gases such as ozone, water vapor, and carbon dioxide (Holton and Wehrbein 1980). Consequently, precise knowledge of the chemical composition of the stratosphere is required for an accurate understanding of the stratospheric thermal structure and mean circulation.

The key role of stratospheric chemistry for *long-term changes* in the stratospheric circulation is also well established. The Antarctic ozone hole has resulted in a colder and stronger Southern Hemisphere (SH) stratospheric polar vortex (Randel and Wu 1999; Waugh et al. 1999) and a poleward shift of the tropospheric westerly jet, which has significant impacts on SH surface climate (Thompson and Solomon 2002; Gillett and Thompson 2003). The effects of Northern Hemisphere (NH) polar ozone depletion on the circulation are in general much weaker, consistent with the relatively small ozone losses there (e.g., Calvo et al. 2015; Stone et al. 2019; Ivy et al. 2017). Changes in atmospheric carbon dioxide have led to a colder stratosphere (Ramaswamy et al. 2001;

Corresponding author: Simchan Yook, simchan.yook@colostate.edu

DOI: 10.1175/JCLI-D-20-0071.1

Shine et al. 2003), and several modeling studies show that greenhouse gases and ozone depleting substances have also strengthened the stratospheric Brewer–Dobson circulation (Butchart and Scaife 2001; Garcia and Randel 2008; Polvani et al. 2019).

The importance of stratospheric chemistry for *internal variability* in the stratospheric circulation remains more uncertain. For example, Smith et al. (2014) compared the mean and variability of the simulated climate in two preindustrial simulations run on the National Center for Atmospheric Research (NCAR) Whole Atmosphere Community Climate Model (WACCM) with varying configurations of chemical process: 1) a ''free-running'' simulation that includes fully coupled chemistry–climate interactions and 2) a ''specified chemistry'' simulation forced with prescribed, annually repeating, climatological-mean chemical composition of ozone and other radiatively active gases [atomic and molecular oxygen (O and O_2), nitrogen oxide (NO), and carbon dioxide (CO_2)] in the middle atmosphere derived from the free-running experiment. Both models are coupled to active ocean, land, and sea ice models. The main conclusion from their work is that prescribing annually repeating values of chemical composition leads to an effectively *identical mean climate* as that found in the coupled simulation. However, they did not explore in detail the role of coupled chemistry in driving the variability in climate about its seasonal cycle throughout the global stratosphere. More recent works have explored the role of feedbacks between chemistry and dynamics for stratosphere–troposphere coupling (Haase and Matthes 2019), for the annual temperature cycle in the lower tropical stratosphere (Fueglistaler et al. 2011; Gilford and Solomon 2017; Ming et al. 2017), and for temperature variability in the polar stratosphere (Rieder et al. 2019). But again, the importance of such feedbacks for temperature variability throughout the global stratosphere has not been quantified.

Here we revisit the so-called free-running and specified chemistry simulations produced with the NCAR WACCM to systematically explore the importance of coupled chemistry interactions for internal climate variability throughout the global stratosphere. A key result of the current study is that the inclusion of coupled chemistry—and thus of variability in ozone about the seasonal cycle—leads to a roughly twofold increase in temperature variability in the lower tropical stratosphere and, to a lesser extent, in the SH polar stratosphere, but relatively modest changes elsewhere. Section 2 provides a description of the climate models, the output used in the analyses, and the analyses methods. Section 3 explores the differences in temperature variance between simulations run with and without coupled chemistry and section 4 probes the connections between stratospheric ozone, radiative heating, and temperature variance. Section 5 provides a discussion and summary of the results.

2. Model and analysis details

a. *WACCM*

We analyze existing 200-yr-long time-slice preindustrial experiments run with two different versions of the Whole Atmosphere Community Climate Model version 4: 1) an experiment run on a free-running, fully coupled chemistry version of the model (FR-WACCM; Marsh et al. 2013) and 2) an experiment run on a version of the model with seasonally varying specified chemistry (SC-WACCM; Smith et al. 2014).

WACCM is the atmospheric component of the National Center for Atmospheric Research (NCAR) Community Earth System Model version 1 (CESM). The chemistry module includes 59 species, 217 gas-phase chemical reactions, 17 heterogeneous reactions on 3 aerosol types, and heating from volcanic aerosols (Marsh et al. 2013). Both the FR-WACCM and SC-WACCM simulations are run with horizontal resolution of $1.9° \times 2.5°$, 66 vertical levels, a model top at approximately 140 km, and identical interactive ocean, land, and sea ice models.

The FR-WACCM simulation was run with 1850 preindustrial emissions, no volcanic forcings, and no quasi-biennial oscillation (QBO). Chemical species such as O_x, NO_x, and HO_x were calculated by the chemistry model. The SC-WACCM simulation is essentially identical in all respects to the FR-WACCM simulation except that 1) the concentrations of ozone are prescribed everywhere and other radiatively active atmospheric constituents (O, O_2, NO, and CO_2) are prescribed in the upper atmosphere (above ~70 km) based on annually repeating, long-term mean values derived from the FR-WACCM run; 2) the concentrations of water vapor and other radiatively active trace gases [e.g., nitrous oxide (N_2O) and methane (CH_4)] in the atmosphere are calculated using the relatively simple Garcia and Solomon two-dimensional model (Garcia and Solomon 1994) rather than fully comprehensive chemistry; and 3) methane oxidation processes in the middle atmosphere are simplified as the conversion of each loss of CH_4 molecule into the production of two water vapor molecules. That is, the long-term, seasonally varying chemical concentrations are identical in the FR-WACCM and SC-WACCM, but only FR-WACCM explicitly simulates the coupling between atmospheric dynamics and chemistry and includes variability in concentrations about the seasonal cycle. More details of the FR-WACCM and SC-WACCM simulations are

provided in Marsh et al. (2013) and Smith et al. (2014), respectively.

b. *Coupled Model Intercomparison Project (CMIP5 and CMIP6) and reanalysis output*

We also analyze output from 1) 13 coupled atmosphere–ocean simulations from the CMIP5 archive run with and without coupled chemistry processes and 2) the Community Atmosphere Model 6 (CAM6) from the CMIP6 archive. The models all extend to at least 1 hPa and are all run with preindustrial forcings. The model output is linearly interpolated to the same 1.9° latitude × 2.5° longitude mesh and pressure levels as the WACCM output.

Observations are derived from the European Centre for Medium-Range Weather Forecasts (ECMWF) interim reanalysis (ERA-Interim; Simmons et al. 2007).

c. *Analysis methods*

We analyze model (WACCM) output of anomalous monthly mean temperature, ozone concentrations, shortwave (SW) heating rates, longwave (LW) heating rates, and vertical velocity. Anomalies are defined as deviations from the long-term mean annual cycle at all grid points. The F statistic is used to assess the statistical significance of the ratios between variances. Area averages are weighted by pressure and cosine of latitude as necessary.

3. Results

Figures 1 and 2 summarize the key differences in ozone and temperature variability between the free-running coupled chemistry (FR) and the specified chemistry (SC) simulations. The top panels show the variances in zonal-mean ozone concentrations in the FR simulation (note that the variances are by construction zero in the SC simulation), the middle panels show the variances in zonal-mean temperature in the FR simulation, and the bottom panels show the ratios of the variances in zonal-mean temperature between the FR and SC simulations. Figure 1 is based on output from all months of the year. Figure 2 highlights results at 60 hPa as a function of calendar month.

Ozone variability in the FR simulation increases markedly with height at stratospheric levels (Fig. 1a). It exhibits two distinct maxima in the middle stratosphere, one at tropical latitudes and another at polar latitudes (Fig. 1a). At the 60 hPa level, variability in polar ozone peaks during the winter months in the Northern Hemisphere and during the late winter/spring months in the Southern Hemisphere (Fig. 2a). Month-to-month variability in tropical ozone peaks during the NH winter months (Fig. 2a), consistent with the season when the wave-driven vertical motion is largest in the tropical stratosphere (Yulaeva et al. 1994; Norton 2006; Randel et al. 2007a; Grise and Thompson 2013).

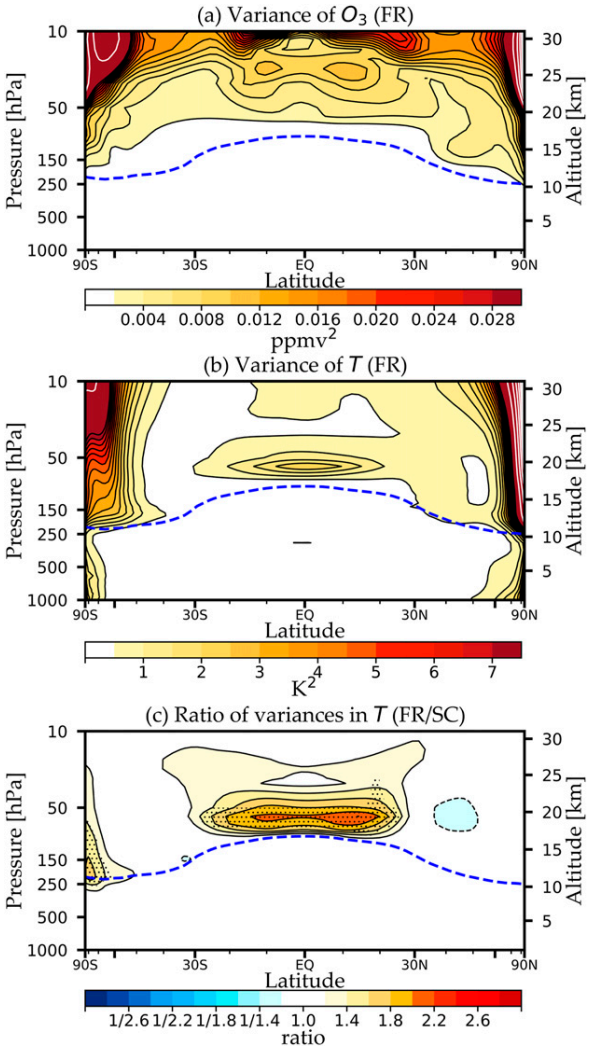

FIG. 1. Variance in zonal-mean (a) ozone concentration and (b) temperature in the free-running coupled chemistry (FR) simulations. (c) Ratios of the variance in zonal-mean temperature between the coupled chemistry (FR) and fixed chemistry (SC) simulations. Stippling indicates regions where the ratios exceed the 95% threshold. The contour intervals with white solid lines are 10 times the contour intervals with black solid lines. The blue dashed line indicates the climatological-mean tropopause height in FR run. The mean tropopause heights in both simulations are effectively identical to each other.

As is the case for ozone, temperature variability in the FR simulation also exhibits distinct maxima in the polar stratosphere and the lower tropical stratosphere (Fig. 1b). Variability in polar temperatures peaks during the winter months in the Northern Hemisphere and during the late winter/spring months in the Southern Hemisphere (Fig. 2b), consistent with the seasonally varying dynamic

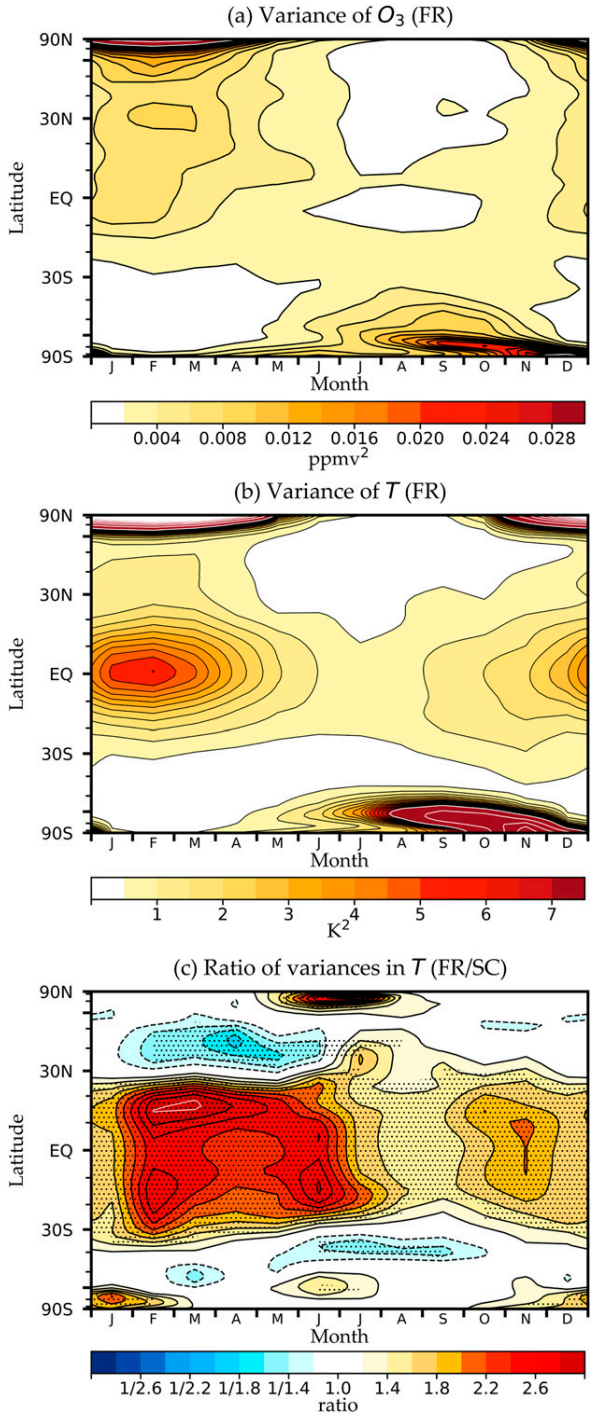

FIG. 2. As in Fig. 1, but for the variance in zonal-mean ozone concentrations and temperature at 60 hPa for each calendar month. In (c) solid (dashed) contours are used for ratio values larger (smaller) than 1.

variability in the high-latitude stratosphere (Andrews et al. 1987). Variability in tropical temperatures peaks during the NH winter months (Fig. 2b), consistent with the seasonally varying dynamic variability in the tropical stratosphere (Yulaeva et al. 1994; Norton 2006; Randel et al. 2007a; Grise and Thompson 2013). The most distinct differences between the patterns of temperature and ozone variance lie at tropical latitudes, where 1) the peak in temperature variance is found at lower altitudes than the peak in ozone variance (Figs. 1a,b) and 2) the temperature variance exhibits a more pronounced tropical maximum (Figs. 2a,b).

The ratios in zonal-mean temperature variance between the FR and SC simulations indicate that coupled chemistry leads to several significant changes in stratospheric temperature variance (Figs. 1c and 2c). By far the most pronounced differences in zonal-mean temperature variance between the FR and SC simulations are found in the lower tropical stratosphere. Coupled chemistry leads to increases in temperature variance of >150% throughout the tropical stratosphere from the tropopause to ~30 hPa and ~200% around the ~70 hPa level (Fig. 1c). The increases in temperature variance in the FR run are highly significant and peak during the NH spring months of February–June, when they approach 300% (Fig. 2c). Weaker but significant temperature variance increases are found in both polar regions during local summer (Fig. 2c), and temperature variance decreases are found in the middle latitudes, particularly during NH spring (Fig. 2c).

Recent work has noted the importance of coupled chemistry for polar stratospheric temperature variability during the spring months (Rieder et al. 2019). The results in Fig. 2 support these findings. But they also indicate that by far the most pronounced effects of coupled chemistry on stratospheric temperature variability are found not in the NH polar stratosphere, but in the lower tropical stratosphere, where temperature variances increase by up to a factor of 3 when coupled chemistry is included in the simulation.

4. Interpretation

Why does coupled chemistry lead to increases in stratospheric temperature variance? FR-WACCM and SC-WACCM differ from each other only in their treatment of atmospheric chemistry. They have identical seasonal cycles, but only FR-WACCM includes intraseasonal and interannual variability in ozone about the seasonal cycle. We hypothesize that the changes in temperature variance with coupled chemistry arise primarily from the changes in both shortwave and longwave heating on dynamically induced variations in ozone.

To test this hypothesis, we show first the temperature variance explained by variations in SW heating rates in the FR simulation. Variations in shortwave heating account for a relatively large fraction of the temperature

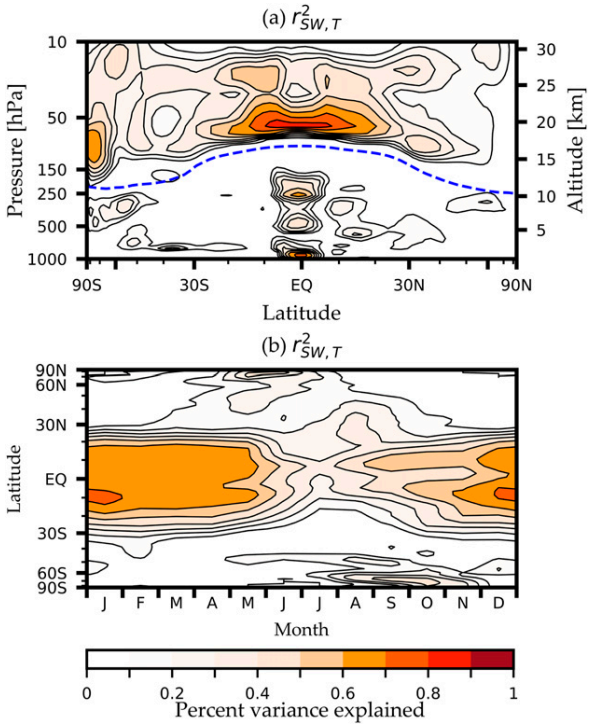

FIG. 3. Percentage of (a) zonal-mean temperature variability explained by variations in the zonal-mean SW heating rates in the FR simulation. (b) As in (a), but for results at 60 hPa as a function of calendar month.

variance in two primary regions: 1) the tropical stratosphere and 2) the SH polar stratosphere during spring (Figs. 3a,b). The correlations are particularly high in the lower tropical stratosphere, where they approach $r = 0.92$ based on 200 years of monthly mean output. In contrast, variations in shortwave heating account for a relatively small fraction of the temperature variance in the midlatitude stratosphere. Figure 3 thus reveals that 1) regions where variations in the SW heating rates explain a large fraction of the variability in the temperature field (Fig. 3a) correspond closely to 2) regions where the inclusion of coupled chemistry leads to increases in the temperature variance (Fig. 1c).

We computed similar results for LW heating (not shown). Variations in LW heating include changes not only in the absorption and emission of longwave radiation by ozone, but also in the longwave emission by all radiatively active gases (the Planck feedback). As discussed below, the changes in absorption and emission of longwave radiation by ozone likely play an important role in setting the vertical structure of the temperature response to coupled chemistry, much as they play an important role in the seasonal cycle of lower-stratospheric temperatures (Gilford and Solomon 2017).

Why are the SW heating rates most closely coupled to stratospheric temperatures in the tropical stratosphere? Variability in SW heating is expected to contribute most to temperature variability in regions where 1) the mean shortwave radiation is large and/or 2) other radiative processes (e.g., longwave radiative relaxation) or dynamical processes (e.g., the eddy transports of heat) do not dominate the thermodynamic energy budget. Both conditions are met in the tropical stratosphere and—to a lesser extent—at high latitudes during the warm-season months. The seasonal cycle of the variances explained by SW heating (Fig. 3b) follows from the seasonal cycle of the ozone variances (Fig. 2a). Within the tropics, dynamically driven variations in vertical motion—and thus ozone—are most pronounced during the NH cold-season months (Fig. 2a; Yulaeva et al. 1994). As such, variations in SW heating account for a larger fraction of variability in temperature during roughly the same season (Fig. 3b).

And why are the SW heating rates more closely coupled to temperatures in the lower stratosphere (i.e., below 50 hPa) than the middle stratosphere? The vertical structures of both 1) the temperature variances explained by SW heating (Fig. 3a) and 2) the increases in temperature variances between the FR and SC simulations (Fig. 1c) are consistent with the competing longwave and shortwave radiative effects of ozone. For example: Consider the tropical stratospheric response to anomalous downward motion. The resulting dynamically induced increases in stratospheric temperatures and ozone should lead to anomalous SW heating through changes in the transmission and absorption of solar radiation, anomalous LW heating due to the absorption of upwelling and downwelling radiation within the 9.6 μm band, and anomalous LW cooling due to increased temperature (Petty 2006; Plass 1956; Kiehl and Solomon 1986; Gilford and Solomon 2017). The different effects are not vertically uniform: Both the SW heating and LW cooling will be larger in the middle stratosphere where ozone concentrations are high, there is more ultraviolet radiation, and there is less absorption overhead. In contrast, the LW heating by ozone will be largest in the lower stratosphere due to increased absorption of 1) upwelling longwave radiation from the troposphere and 2) downwelling longwave radiation from the middle stratosphere. As a result of the above, LW cooling due to ozone is more effective at damping temperature changes in the middle stratosphere than it is in the lowermost stratosphere, and the net radiative effects of ozone variability on stratospheric temperatures should be most pronounced in the lower stratosphere (e.g., see also Forster and Shine 1997; Fels et al. 1980).

To analyze the influence of dynamically driven ozone variability on the stratospheric temperature, we regressed zonal-mean temperature, ozone, SW heating rates, and LW heating rates against a simple index that measures the dynamical upwelling in the tropical stratosphere (Figs. 4 and 5). Recall that the LW heating rates include both the effects of changes in emissivity and temperature, and thus the LW fluxes shown below include changes in both 1) absorption and emission of both upwelling and longwave radiation within the 9.6 μm band and 2) the Planck feedback.

The tropical upwelling index was formed as follows:

1) The Eulerian-mean vertical velocity was averaged over 20°S–20°N and between the 100 and 10 hPa levels as a function of calendar month to form a time series $w(t)$ of tropical stratospheric vertical velocity, where t denotes each month.
2) The lag between tropical upwelling and stratospheric temperatures (Newman and Rosenfield 1997; Randel et al. 2002; Ueyama and Wallace 2010) was accounted for by averaging consecutive values of the resulting monthly-mean vertical velocity time series, such that $W(t) = (2/3)w(t - 1) + (1/3)w(t)$, where $W(t)$ is the tropical upwelling index.
3) The resulting tropical upwelling index $W(t)$ values were standardized so that a unit change in the index corresponds to a typical fluctuation in tropical stratospheric vertical velocity.

Note that the tropical upwelling index $W(t)$ is defined as an average of vertical velocity in pressure coordinates. Thus, positive values of the index correspond to anomalous downward motion, and vice versa.

In practice, the tropical upwelling index can be recovered as a linear combination of the first two principal components of tropical stratospheric vertical velocity anomalies in both SC and FR, which explain more than 95% of the variability in the tropical stratospheric vertical velocity field.

Figures 4 and 5 explore the differences in radiative effects between FR and SC associated with a typical fluctuation in tropical upwelling. The top panels show the differences between 1) temperature regressed on $W(t)$ in FR-WACCM and 2) temperature regressed on $W(t)$ in SC-WACCM. Subsequent panels show comparable results for ozone concentrations, SW heating rates, and LW heating rates, respectively. Figure 4 shows results for all months of the year. Figure 5 highlights results at 60 hPa as a function of calendar month.

Anomalous sinking motion in the tropics [i.e., positive values of the tropical upwelling index $W(t)$] leads to larger increases in atmospheric temperatures due to adiabatic warming in FR than it does in SC, as evidenced

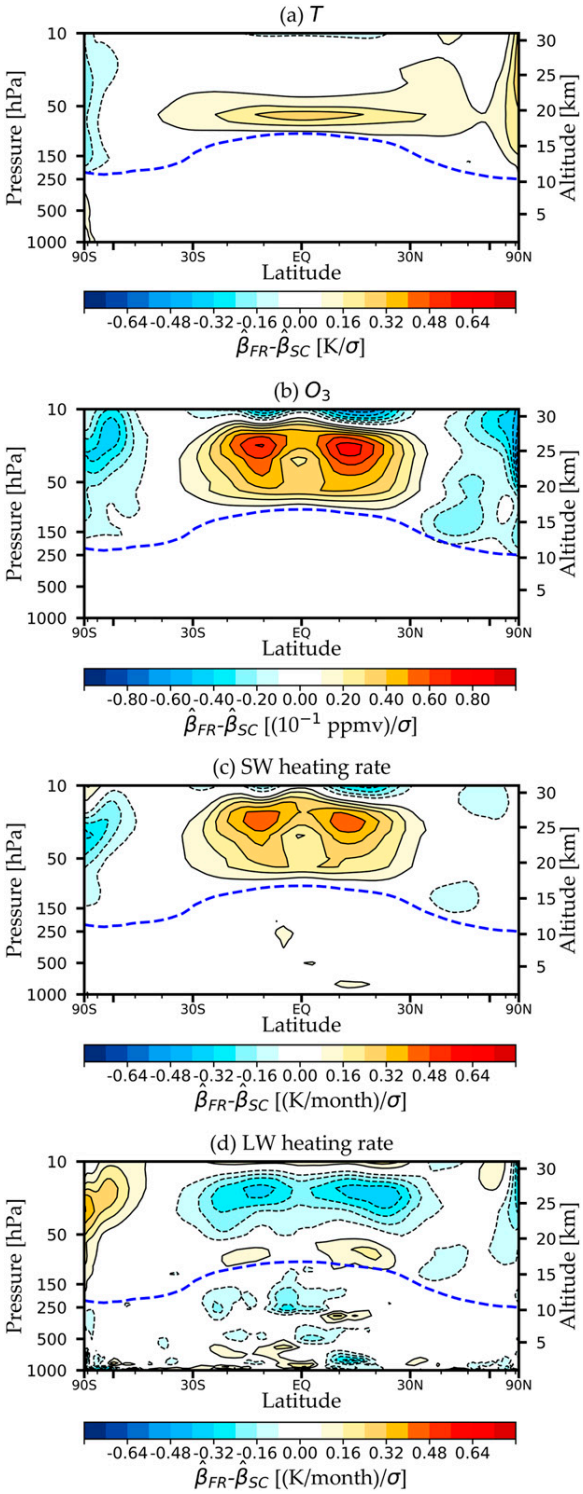

FIG. 4. Differences between regressions on an index of tropical upwelling in the FR and SC simulations. Rows correspond to the differences in regression coefficients for (a) temperature, (b) ozone, (c) SW heating rate, and (d) LW heating rate. Results are based on output for all calendar months.

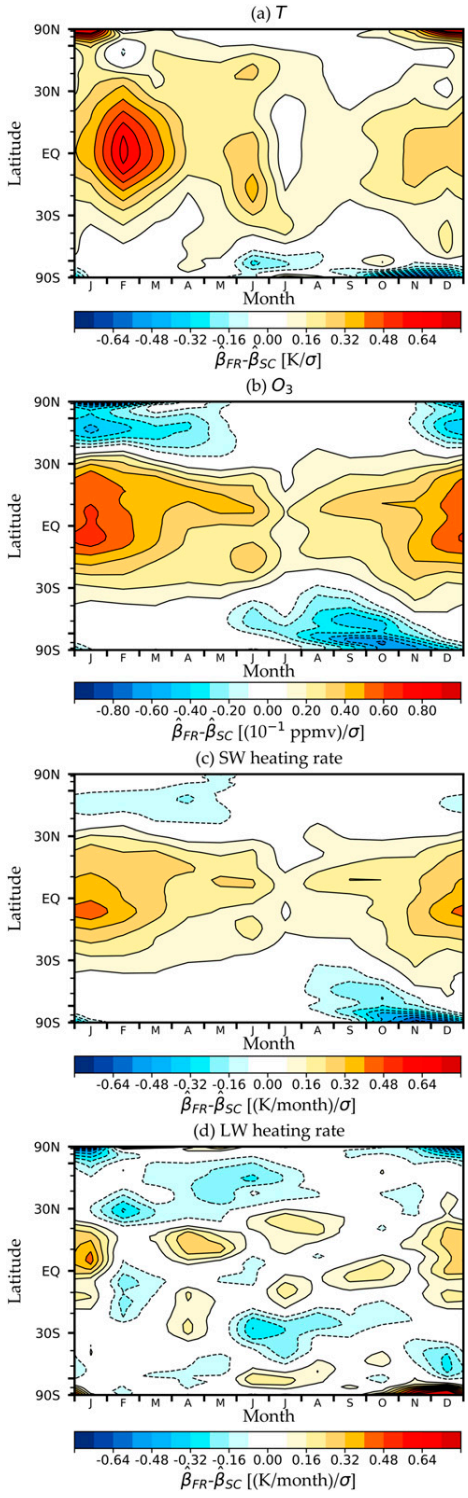

FIG. 5. As in Fig. 4, but for the results at 60 hPa for each calendar month.

by the differences in the regression coefficients shown in the top panels in Figs. 4 and 5. The larger temperature response in FR is primarily confined to the lower stratosphere at tropical latitudes (Fig. 4a). The temperature anomalies associated with a typical fluctuation in vertical motion in FR exceed those in SC by up to 0.6 K month^{-1} σ^{-1} (Fig. 5a). The most pronounced differences between the regression patterns of temperature (Fig. 5a) are found in the tropics during the NH winter months.

Anomalous downwelling in the tropical stratosphere is accompanied by widespread increases in ozone concentrations throughout the lower and middle tropical stratosphere below ~15 hPa (Fig. 4b). Note that since there is no ozone variability in SC, the results in Figs. 4b and 5b are equivalent to the regressions for FR since the regression coefficients for SC are zero everywhere. The increases in ozone are consistent with anomalous downward transport of high-ozone air from upper levels. Like the differences in temperature variations between the coupled and specified chemistry simulations, they also peak during the NH cold-season months (Fig. 5b). Unlike the differences in temperature variations between the coupled and specified chemistry simulations, the differences in ozone peak in middle stratosphere ~30 hPa rather than ~70 hPa. The decreases in ozone in the tropical stratosphere above ~15 hPa are consistent with the facts that 1) ozone is controlled primarily by photochemistry rather than transport there, and 2) warming due to anomalous downwelling leads to decreases in ozone through changes in the gas-phase catalytic destruction of ozone (e.g., Fusco and Salby 1999; Eyring et al. 2010). The decreases in ozone at high latitudes reflect the fact that anomalous downwelling in the tropical stratosphere is accompanied by anomalous upwelling at latitudes (vertical motion at high latitudes is not shown).

The differences in SW heating rates between periods of tropical downwelling in the FR-WACCM and SC-WACCM simulations (Figs. 4c and 5c) are qualitatively very similar to the differences in ozone (Figs. 4b and 5b). At first glance, the differences in LW heating rates (Figs. 4d and 5d) bear close resemblance to the differences in ozone variability. However, closer inspection reveals that the anomalous cooling due to enhanced emission of longwave radiation is confined to levels above about 50 hPa. That is, anomalous LW cooling opposes anomalous SW heating at levels above ~50 hPa but is approximately zero or even weakly positive in the lower tropical stratosphere (Figs. 4d and 5d). The vertical structure of the differences in LW heating is consistent with the physical reasoning outlined earlier, namely that 1) the Planck feedback is more efficient

at higher levels, where the opacity of the overlying atmosphere is smaller (Hitchcock et al. 2010); and 2) the increased absorption of both downwelling and upwelling longwave radiation by ozone should be largest in the lower stratosphere, as is the case in the seasonal cycle there (Gilford and Solomon 2017).

Together, the results in Figs. 4 and 5 suggest that the inclusion of ozone variability in coupled chemistry simulations is most effective at increasing the temperature variance in the lower tropical stratosphere since LW radiative cooling is less effective at opposing radiative heating there. The vertical profile of the increases in temperature variance due to coupled chemistry is thus consistent with our understanding of the radiative balance in the lower stratosphere and its relatively long radiative time scales (e.g., Forster and Shine 1997; Fels et al. 1980; Hitchcock et al. 2010). In fact, consistent with our hypothesis, coupled chemistry leads to marked increases not only in lower tropical stratospheric temperature variance, but also in the memory in lower tropical stratospheric temperatures from one month to the next (Fig. 6).

Previous studies have suggested that dynamical feedbacks other than the ozone–radiation feedback highlighted here may affect tropical stratospheric temperature variability. For example, changes in the stratification of the atmosphere affect vertical motion and its influence on adiabatic temperature change (Birner and Charlesworth 2017; Fueglistaler et al. 2011), and variations in the dynamical and radiative time scales affect stratospheric temperature variance (Charlesworth et al. 2019). Importantly, the differences in stratospheric temperature variance revealed here do not seem to derive from changes in the variance of stratospheric dynamics, that is, the variance of the temperature tendency due to vertical motion (ωS) is roughly unchanged in the tropical stratosphere between the FR and SC-WACCM simulations (not shown).

The results indicated in Figs. 1–5 also appear to extend to simulations used in the AR5 and AR6 reports. Figure 7 compares the lower-stratospheric temperature variance in FR-WACCM and SC-WACCM with that found in the observations (ERA-Interim), a range of high-top CMIP5 models, and output from the low-top version of the NCAR Community Atmospheric Model (CAM6) used in the AR6 report. The high-top models are grouped into two different categories: 1) models with a parameterized QBO (shown at left) and 2) models without a QBO (right). The temperature variances are found in model output by 1) forming temperature anomalies by removing the long-term mean seasonal cycle from the output, 2) averaging the anomalies over the region 30°S–30°N and 70–50 hPa, and then

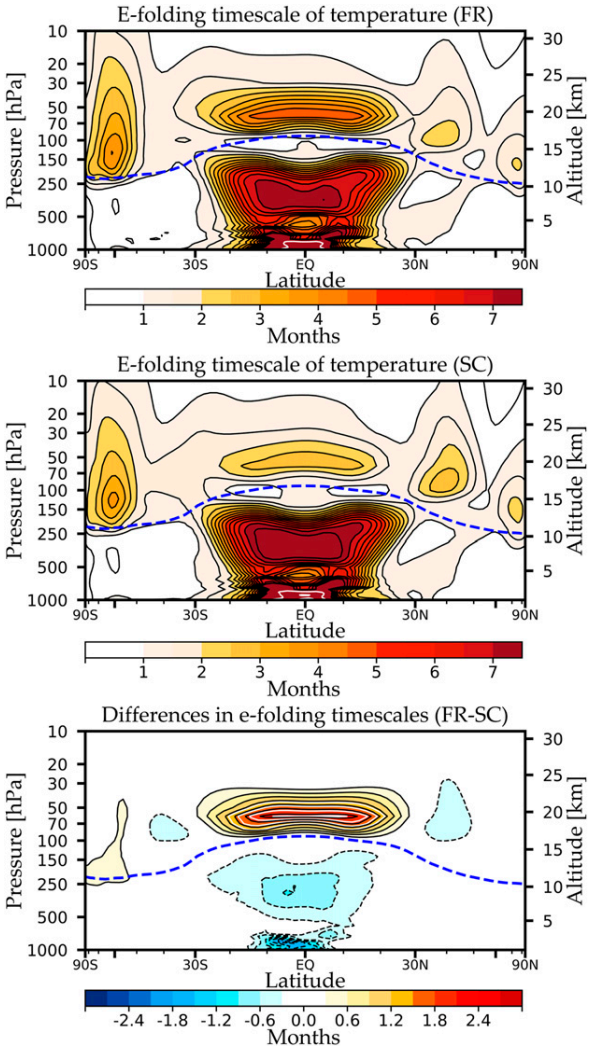

FIG. 6. The *e*-folding time scale of zonal-mean temperature anomalies in (top) the coupled chemistry simulation (FR) and (middle) the prescribed chemistry simulation (SC), and (bottom) the differences between FR and SC.

3) computing the variances of the spatially averaged temperature time series. The observed variance is found in a similar manner, except that we also remove the influence of volcanic eruptions since they are not included in the numerical output. The influence of volcanic eruptions on lower-stratospheric temperature variance is mitigated by excluding data during 1982–84 and 1991–93 (i.e., the years surrounding the eruptions of El Chichón and Mount Pinatubo, respectively).

Together, the results in Fig. 7 reveal that 1) models with interactive chemistry (FR-WACCM, GFDL-CM3, and MIROC-ESM-CHEM) all indicate larger tropical stratospheric temperature variances than models with prescribed chemistry, when the output is binned by

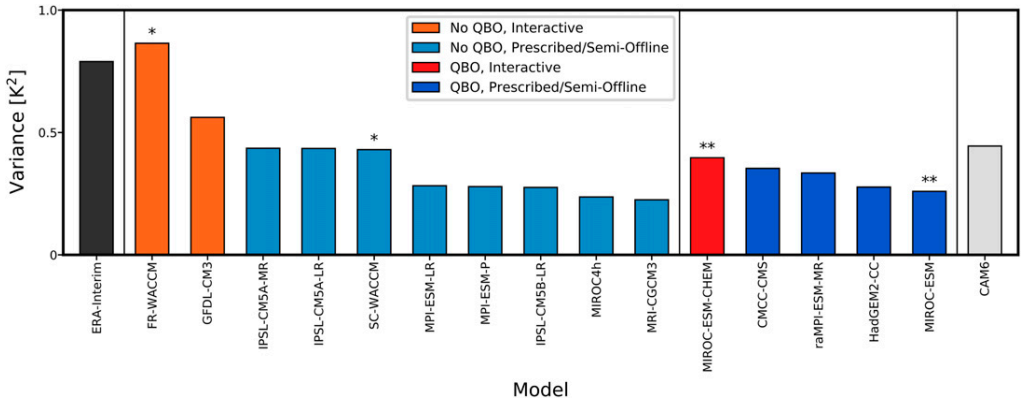

FIG. 7. The temperature variances in the lower tropical stratosphere in the observations (ERA-Interim), high-top models from the CMIP5 archive, and CAM6 from the CMIP6 archive. Orange- and red-colored bars denote models with interactive chemistry, while cyan- and blue-colored bars denote models with prescribed chemistry. Orange and cyan bars denote models with a QBO parameterization, while red and blue bars denote models without QBO parameterization. The black bar denotes ERA-Interim and the gray bar denotes CAM6.

model treatments of the QBO; 2) the tropical stratospheric temperature variance in the coupled chemistry version of WACCM (FR) is very similar to the observed, whereas the variance in the prescribed chemistry version (SC) notably underestimates the observations (Fig. 7); and 3) the tropical stratospheric variance in CAM6 (far right bar in Fig. 7) is similar to that found in the prescribed chemistry version of WACCM, and thus also significantly underestimates the observations.

5. Discussion

Previous studies have suggested that "the climatology and variability of the stratosphere ... are nearly identical" in simulations run on coupled and prescribed chemistry versions of the NCAR Whole Atmosphere Community Climate Model (Smith et al. 2014, p. 883). The results shown here indicate that, in fact, coupled climate–chemistry interactions play an *essential* role in driving temperature variability in the tropical lower stratosphere and—to a lesser extent—the polar regions during summer. In the tropical lower stratosphere, simulations with explicit interactions between dynamics, ozone, and radiation indicate approximately twofold increases in month-to-month temperature variability relative to simulations with prescribed chemistry. The increases in lower tropical stratospheric temperature variance are consistent with the changes in shortwave and longwave radiative heating rates that accompany dynamically driven ozone variability in tropical stratosphere. The variance increases are most pronounced in the lowermost stratosphere where 1) heating due to the absorption of both upwelling and downwelling longwave radiation are important (Gilford and Solomon 2017) and 2) longwave radiative cooling is relatively inefficient at damping temperature variability on monthly time scales.

The conclusions are drawn from analyses of 200-yr-long simulations run on two different versions of the WACCM: 1) a fully coupled chemistry version of the model (FR-WACCM; Marsh et al. 2013) and 2) a specified chemistry version of the model (SC-WACCM; Smith et al. 2014). Importantly, they also extend to models run for IPCC AR5: lower-stratospheric temperature variability is consistently larger in models with interactive chemistry relative to models with prescribed chemistry. Hence the results indicate the critical role of explicitly simulated coupled chemistry interactions for the fidelity of simulating stratospheric climate variability in climate change simulations.

Variations in lower tropical stratospheric temperatures play an outsized role in global climate variability (e.g., Fueglistaler et al. 2011). They set the amplitude of stratospheric water vapor concentrations (Brewer 1949; Fueglistaler et al. 2009), which, in turn, play a key role in the radiative forcing at the tropopause (Forster and Shine 1999). The climatological-mean seasonal cycle of water vapor in the tropical upper troposphere–lower stratosphere region is well simulated in both FR-WACCM and SC-WACCM (Smith et al. 2014). However, in contrast to ozone, water vapor is not strictly prescribed in the SC simulation. For example, like ozone, stratospheric water vapor concentrations in FR-WACCM are calculated using prognostic chemistry. However, unlike ozone, stratospheric water vapor concentrations in SC-WACCM are not prescribed from

annually repeating values, but rather are calculated including approximate methane oxidation and photolysis rates, and transport. Hence, it is difficult to use the differences between FR-WACCM and SC-WACCM to assess the role of coupled chemistry on stratospheric water vapor variability. We view it as critical for future work to quantify the importance of the nearly twofold increase in temperature variability documented here for stratospheric water vapor and the resulting radiative forcing of the tropopause as well as its possible influences on tropospheric climate.

Acknowledgments. The authors thank Stephan Fueglistaler and two anonymous reviewers for their helpful comments on the manuscript. D.W.J.T. and S.Y. are partly funded by NSF Climate and Large-Scale Dynamics (AGS-1848785). S.S. is partly supported by NSF Climate and Large-Scale Dynamics (AGS-1848863). The CESM project is supported by the NSF and the Office of Science (BER) of the U.S. Department of Energy (DOE). The authors acknowledge the Climate Simulation Laboratory at NCAR's Computational and Information Systems Laboratory (CISL; sponsored by NSF and other agencies) and the NOAA Research and Development High Performance Computing Program for providing computing and storage resources that have contributed to the research results reported within this paper.

REFERENCES

Andrews, D. G., C. B. Leovy, and J. R. Holton, 1987: *Middle Atmosphere Dynamics.* Academic Press, 489 pp.

Birner, T., 2006: Fine-scale structure of the extratropical tropopause region. *J. Geophys. Res.*, **111**, D04104, https://doi.org/10.1029/2005JD006301.

——, and E. J. Charlesworth, 2017: On the relative importance of radiative and dynamical heating for tropical tropopause temperatures. *J. Geophys. Res. Atmos.*, **122**, 6782–6797, https://doi.org/10.1002/2016JD026445.

Brasseur, G. P., and S. Solomon, 2005: *Aeronomy of the Middle Atmosphere*. Springer, 646 pp.

Brewer, A., 1949: Evidence for a world circulation provided by the measurements of helium and water vapour distribution in the stratosphere. *Quart. J. Roy. Meteor. Soc.*, **75**, 351–363, https://doi.org/10.1002/qj.49707532603.

Butchart, N., and A. A. Scaife, 2001: Removal of chlorofluorocarbons by increased mass exchange between the stratosphere and troposphere in a changing climate. *Nature*, **410**, 799–802, https://doi.org/10.1038/35071047.

Calvo, N., L. M. Polvani, and S. Solomon, 2015: On the surface impact of Arctic stratospheric ozone extremes. *Environ. Res. Lett.*, **10**, 094003, https://doi.org/10.1088/1748-9326/10/9/094003.

Charlesworth, E. J., T. Birner, and J. R. Albers, 2019: Ozone transport–radiation feedbacks in the tropical tropopause layer. *Geophys. Res. Lett.*, **46**, 14 195–14 202, https://doi.org/10.1029/2019GL084679.

Eyring, V., and Coauthors, 2010: Multi-model assessment of stratospheric ozone return dates and ozone recovery in CCMVal-2 models. *Atmos. Chem. Phys.*, **10**, 9451–9472, https://doi.org/10.5194/acp-10-9451-2010.

Fels, S., J. Mahlman, M. Schwarzkopf, and R. Sinclair, 1980: Stratospheric sensitivity to perturbations in ozone and carbon dioxide: Radiative and dynamical response. *J. Atmos. Sci.*, **37**, 2265–2297, https://doi.org/10.1175/1520-0469(1980)037<2265:SSTPIO>2.0.CO;2.

Forster, P. M., and K. P. Shine, 1997: Radiative forcing and temperature trends from stratospheric ozone changes. *J. Geophys. Res.*, **102**, 10 841–10 855, https://doi.org/10.1029/96JD03510.

——, and ——, 1999: Stratospheric water vapour changes as a possible contributor to observed stratospheric cooling. *Geophys. Res. Lett.*, **26**, 3309–3312, https://doi.org/10.1029/1999GL010487.

——, and ——, 2002: Assessing the climate impact of trends in stratospheric water vapor. *Geophys. Res. Lett.*, **29**, 1086, https://doi.org/10.1029/2001GL013909.

Fueglistaler, S., A. Dessler, T. Dunkerton, I. Folkins, Q. Fu, and P. W. Mote, 2009: Tropical tropopause layer. *Rev. Geophys.*, **47**, RG1004, https://doi.org/10.1029/2008RG000267.

——, P. Haynes, and P. Forster, 2011: The annual cycle in lower stratospheric temperatures revisited. *Atmos. Chem. Phys.*, **11**, 3701–3711, https://doi.org/10.5194/acp-11-3701-2011.

Fusco, A. C., and M. L. Salby, 1999: Interannual variations of total ozone and their relationship to variations of planetary wave activity. *J. Climate*, **12**, 1619–1629, https://doi.org/10.1175/1520-0442(1999)012<1619:IVOTOA>2.0.CO;2.

Garcia, R. R., and S. Solomon, 1994: A new numerical model of the middle atmosphere: 2. Ozone and related species. *J. Geophys. Res.*, **99**, 12 937–12 951, https://doi.org/10.1029/94JD00725.

——, and W. J. Randel, 2008: Acceleration of the Brewer–Dobson circulation due to increases in greenhouse gases. *J. Atmos. Sci.*, **65**, 2731–2739, https://doi.org/10.1175/2008JAS2712.1.

Gilford, D. M., and S. Solomon, 2017: Radiative effects of stratospheric seasonal cycles in the tropical upper troposphere and lower stratosphere. *J. Climate*, **30**, 2769–2783, https://doi.org/10.1175/JCLI-D-16-0633.1.

Gillett, N. P., and D. W. Thompson, 2003: Simulation of recent Southern Hemisphere climate change. *Science*, **302**, 273–275, https://doi.org/10.1126/science.1087440.

Grise, K. M., and D. W. Thompson, 2013: On the signatures of equatorial and extratropical wave forcing in tropical tropopause layer temperatures. *J. Atmos. Sci.*, **70**, 1084–1102, https://doi.org/10.1175/JAS-D-12-0163.1.

Haase, S., and K. Matthes, 2019: The importance of interactive chemistry for stratosphere–troposphere coupling. *Atmos. Chem. Phys.*, **19**, 3417–3432, https://doi.org/10.5194/acp-19-3417-2019.

Hitchcock, P., T. G. Shepherd, and S. Yoden, 2010: On the approximation of local and linear radiative damping in the middle atmosphere. *J. Atmos. Sci.*, **67**, 2070–2085, https://doi.org/10.1175/2009JAS3286.1.

Holton, J. R., and W. M. Wehrbein, 1980: A numerical model of the zonal mean circulation of the middle atmosphere. *Pure Appl. Geophys.*, **118**, 284–306, https://doi.org/10.1007/BF01586455.

Ivy, D. J., S. Solomon, N. Calvo, and D. W. Thompson, 2017: Observed connections of Arctic stratospheric ozone extremes to Northern Hemisphere surface climate. *Environ. Res. Lett.*, **12**, 024004, https://doi.org/10.1088/1748-9326/aa57a4.

Kiehl, J., and S. Solomon, 1986: On the radiative balance of the stratosphere. *J. Atmos. Sci.*, **43**, 1525–1534, https://doi.org/10.1175/1520-0469(1986)043<1525:OTRBOT>2.0.CO;2.

Marsh, D. R., M. J. Mills, D. E. Kinnison, J.-F. Lamarque, N. Calvo, and L. M. Polvani, 2013: Climate change from 1850

to 2005 simulated in CESM1(WACCM). *J. Climate*, **26**, 7372–7391, https://doi.org/10.1175/JCLI-D-12-00558.1.

Ming, A., A. C. Maycock, P. Hitchcock, and P. Haynes, 2017: The radiative role of ozone and water vapour in the annual temperature cycle in the tropical tropopause layer. *Atmos. Chem. Phys.*, **17**, 5677–5701, https://doi.org/10.5194/acp-17-5677-2017.

Newman, P. A., and J. E. Rosenfield, 1997: Stratospheric thermal damping times. *Geophys. Res. Lett.*, **24**, 433–436, https://doi.org/10.1029/96GL03720.

Norton, W., 2006: Tropical wave driving of the annual cycle in tropical tropopause temperatures. Part II: Model results. *J. Atmos. Sci.*, **63**, 1420–1431, https://doi.org/10.1175/JAS3698.1.

Petty, G. W., 2006: *A First Course in Atmospheric Radiation*. Sundog Publishing, 459 pp.

Plass, G. N., 1956: The influence of the 9.6 micron ozone band on the atmospheric infra-red cooling rate. *Quart. J. Roy. Meteor. Soc.*, **82**, 30–44, https://doi.org/10.1002/qj.49708235104.

Polvani, L. M., and Coauthors, 2019: Large impacts, past and future, of ozone-depleting substances on Brewer-Dobson circulation trends: A multimodel assessment. *J. Geophys. Res. Atmos.*, **124**, 6669–6680, https://doi.org/10.1029/2018JD029516.

Ramaswamy, V., and Coauthors, 2001: Stratospheric temperature trends: Observations and model simulations. *Rev. Geophys.*, **39**, 71–122, https://doi.org/10.1029/1999RG000065.

Randel, W. J., and F. Wu, 1999: Cooling of the Arctic and Antarctic polar stratospheres due to ozone depletion. *J. Climate*, **12**, 1467–1479, https://doi.org/10.1175/1520-0442(1999)012<1467:COTAAA>2.0.CO;2.

——, R. R. Garcia, and F. Wu, 2002: Time-dependent upwelling in the tropical lower stratosphere estimated from the zonal-mean momentum budget. *J. Atmos. Sci.*, **59**, 2141–2152, https://doi.org/10.1175/1520-0469(2002)059<2141:TDUITT>2.0.CO;2.

——, M. Park, F. Wu, and N. Livesey, 2007a: A large annual cycle in ozone above the tropical tropopause linked to the Brewer–Dobson circulation. *J. Atmos. Sci.*, **64**, 4479–4488, https://doi.org/10.1175/2007JAS2409.1.

——, F. Wu, and P. Forster, 2007b: The extratropical tropopause inversion layer: Global observations with GPS data, and a radiative forcing mechanism. *J. Atmos. Sci.*, **64**, 4489–4496, https://doi.org/10.1175/2007JAS2412.1.

Rieder, H. E., G. Chiodo, J. Fritzer, C. Wienerroither, and L. M. Polvani, 2019: Is interactive ozone chemistry important to represent polar cap stratospheric temperature variability in Earth-System Models? *Environ. Res. Lett.*, **14**, 044026, https://doi.org/10.1088/1748-9326/ab07ff.

Shine, K. P., and Coauthors, 2003: A comparison of model-simulated trends in stratospheric temperatures. *Quart. J. Roy. Meteor. Soc.*, **129**, 1565–1588, https://doi.org/10.1256/qj.02.186.

Simmons, A., S. Uppala, D. Dee, and S. Kobayashi, 2007: ERA-Interim: New ECMWF reanalysis products from 1989 onwards. *ECMWF Newsletter*, No. 110, ECMWF, Reading, United Kingdom, 25–35, https://www.ecmwf.int/sites/default/files/elibrary/2007/17713-era-interim-new-ecmwf-reanalysis-products-1989-onwards.pdf.

Smith, K. L., R. Neely, D. Marsh, and L. M. Polvani, 2014: The Specified Chemistry Whole Atmosphere Community Climate Model (SC-WACCM). *J. Adv. Model. Earth Syst.*, **6**, 883–901, https://doi.org/10.1002/2014MS000346.

Stone, K. A., S. Solomon, D. E. Kinnison, C. F. Baggett, and E. A. Barnes, 2019: Prediction of Northern Hemisphere regional surface temperatures using stratospheric ozone information. *J. Geophys. Res. Atmos.*, **124**, 5922–5933, https://doi.org/10.1029/2018JD029626.

Thompson, D. W., and S. Solomon, 2002: Interpretation of recent Southern Hemisphere climate change. *Science*, **296**, 895–899, https://doi.org/10.1126/science.1069270.

Ueyama, R., and J. M. Wallace, 2010: To what extent does high-latitude wave forcing drive tropical upwelling in the Brewer–Dobson circulation? *J. Atmos. Sci.*, **67**, 1232–1246, https://doi.org/10.1175/2009JAS3216.1.

Waugh, D. W., W. J. Randel, S. Pawson, P. A. Newman, and E. R. Nash, 1999: Persistence of the lower stratospheric polar vortices. *J. Geophys. Res.*, **104**, 27 191–27 201, https://doi.org/10.1029/1999JD900795.

Yulaeva, E., J. R. Holton, and J. M. Wallace, 1994: On the cause of the annual cycle in tropical lower-stratospheric temperatures. *J. Atmos. Sci.*, **51**, 169–174, https://doi.org/10.1175/1520-0469(1994)051<0169:OTCOTA>2.0.CO;2.